

## Magnetism in the dilute Kondo lattice model

M. Gulacsi and I. P. McCulloch\*

*Department of Theoretical Physics, Institute of Advanced Studies, The Australian National University, Canberra ACT 0200, Australia*

A. Juozapavicius and A. Rosengren

*Condensed Matter Theory, AlbaNova University Center, Royal Institute of Technology, SE-106 91, Stockholm, Sweden*

(Received 15 October 2003; revised manuscript received 21 January 2004; published 26 May 2004)

The one-dimensional dilute Kondo lattice model is investigated by means of bosonization for different dilution patterns of the array of impurity spins. The physical picture is very different if a commensurate or incommensurate doping of the impurity spins is considered. For the commensurate case, the obtained phase diagram is verified using a non-Abelian density-matrix renormalization-group algorithm. The paramagnetic phase widens at the expense of the ferromagnetic phase as the  $f$  spins are diluted. For the incommensurate case, short-range antiferromagnetic correlations are found to dominate at low doping, which distinguishes the dilute Kondo lattice model from the standard Kondo lattice model.

DOI: 10.1103/PhysRevB.69.174425

PACS number(s): 75.10.Jm, 75.40.Mg, 05.50.+q

Heavy fermion systems have been of great theoretical interest since their discovery some 20 years ago.<sup>1</sup> The central problem posed by heavy fermion materials is to understand the interaction between an array of localized moments (generally  $f$  electrons in lanthanide or actinide ions) and conduction electrons (generally  $s$  or  $d$  band). This situation is well described by an antiferromagnetically coupled Kondo-type model.

The solution of Kondo-type models is well understood in two limiting cases; the single-impurity limit<sup>2</sup> which can be reduced to a one-dimensional problem and solved via Bethe ansatz, and second the Kondo lattice model (KLM), which was solved via bosonization<sup>3</sup> and numerous numerical approaches<sup>4,5</sup> in one dimension for half filling and partial conduction-band filling. For half filling the results indicate the existence of a finite spin and charge gap. Accordingly in this case the Kondo lattice model is an insulator with well-defined massive solitonic excitations of the spin sector.

For partial conduction-band filling, the conduction electrons form a Luttinger liquid, with spin and charge separation.<sup>5</sup> The localized spins, however, exhibit ferromagnetism, due to an effective double-exchange coupling.<sup>3,4</sup> The double exchange is driving the system toward ferromagnetism, while the fluctuations generated by Kondo singlets compete against this tendency. As a consequence, the paramagnetic to ferromagnetic phase transition is of the quantum order-disorder type, typical to models with an effective random field.<sup>3</sup> However, for small Kondo coupling and close to half filling a Ruderman-Kittel-Kasuya-Yosida liquid state and polaronic regime are always present.<sup>4</sup> For additional properties, see earlier reviews of Ref. 6.

Beyond these two solvable limits, no rigorous results exist for the intermediate cases, where the number of impurities are neither one nor equal to the number of sites. This is the focus of our study. We concentrate on the one-dimensional case, and start from the Kondo lattice limit introducing impurity spin holes, that is, we will be dealing with a dilute Kondo lattice model (DKLM):

$$H = -t \sum_{i=1, \sigma}^{L-1} (c_{i, \sigma}^{\dagger} c_{i+1, \sigma} + \text{H.c.}) + J \sum_{i=1}^L \mathcal{P} \mathbf{S}_i^z \cdot \mathbf{S}_i^z, \quad (1)$$

where  $L$  is the number of sites and  $t > 0$  is the conduction electron hopping. We measure the Kondo coupling  $J$  in units of the hopping  $t$ . We denote by  $N_f$  ( $n_f = N_f/L$ ) the number (concentration) of impurities and by  $N_c$  ( $n_c = N_c/L$ ) the number (concentration) of conduction electrons. The constraint  $N_f \leq L$  is imposed by  $\mathcal{P}$ , which is an operator that projects out a predetermined set of  $f$  spins.  $\mathbf{S}_i$  are spin 1/2 operators for the localized spins, e.g.,  $f$ , and  $\mathbf{S}_i^z = \frac{1}{2} \sum_{\sigma, \sigma'} c_{i, \sigma}^{\dagger} \boldsymbol{\sigma}_{\sigma, \sigma'} c_{i, \sigma'}$  with  $\boldsymbol{\sigma}$  the Pauli spin matrices and  $c_{i, \sigma}^{\dagger}$ ,  $c_{i, \sigma}$  the electron creation and annihilation site operators.

We investigate the behavior of the DKLM both by an analytical approach, based on a standard bosonization scheme, and by numerical calculations. The latter were performed using the newly developed non-Abelian density-matrix renormalization-group (DMRG) algorithm,<sup>7</sup> which preserves the total spin and pseudospin symmetry. This choice of basis first of all greatly facilitates the observation of magnetic phases and second it gives a dramatic performance improvement compared to the standard DMRG basis.

The bosonization we use takes the standard approach<sup>8</sup> by first decomposing the on-site operators into Dirac fields, with spinor components  $\tau = \pm$  (otherwise known as the right,  $\tau = +$ , and left,  $\tau = -$ , movers):  $c_{x, \sigma} \approx \sum_{\tau} c_{\tau, x, \sigma} \equiv \sum_{\tau} e^{ik_F x} \Psi_{\tau, \sigma}(x)$ , where  $k_F = \pi n_c/2$  and we consider the lattice spacing to be unity. Next we bosonize the Dirac fields with  $\Psi_{\tau, \sigma} = \exp(i\Phi_{\tau, \sigma})/\sqrt{2\pi\lambda}$ , where  $1/\lambda$  is the ultraviolet cutoff. For the scalar Bose fields,  $\Phi_{\tau, \sigma}(x)$  and its canonical conjugate momenta,  $\Pi_{\tau, \sigma}(x)$ ,  $\Phi_{\tau, \sigma}(x) = \int_{-\infty}^x dx' \Pi_{\tau, \sigma}(x')$ , we use the standard Mandelstam representation,<sup>9</sup> which introduces a momentum cutoff function  $\Lambda(k) = \exp(-\lambda|k|/2)$  via the Fourier transforms. Thus, the electron field can be represented in terms of collective density operators which satisfy Bose commutation relations

$$c_{\tau, x, \sigma} \approx \exp(i\tau k_F x) \exp\{i[\theta_{\rho}(x) + \tau\phi_{\rho}(x) + \sigma[\theta_{\sigma}(x) + \tau\phi_{\sigma}(x)]]/2\}, \quad (2)$$

where the Bose fields (for both  $\nu = \rho, \sigma$ ) are defined by  $\phi_{\nu}/\theta_{\nu} = i(\pi/N) \sum_{k \neq 0} e^{ikx} [\nu_{+}(k) \pm \nu_{-}(k)] \Lambda(k)/k$ , where  $\phi_{\nu}$

are the number fields and  $\theta_\nu$  the current fields. The charge (holon) and spin (spinon) number fluctuations are defined as  $\rho_\tau(k) = \sum_\sigma \rho_{\tau,\sigma}(k)$ , and  $\sigma_\tau(k) = \sum_\sigma \sigma \rho_{\tau,\sigma}(k)$ . This type of Bose representation provides a nonperturbative description of the conduction electrons in terms of holons and spinons.<sup>8</sup> We will neglect for the moment all the rapidly oscillating (umklapp) terms. These will give a contribution only at half filling, i.e.,  $n_c = n_f$ , and will be analyzed later on. Thus, the bosonized form of DKLM is

$$\begin{aligned}
H = & \frac{v_F}{4\pi} \sum_{j,\nu} \{ \Pi_\nu^2(j) + [\partial_x \phi_\nu(j)]^2 \} \\
& + \frac{J}{2\pi} \sum_j [\partial_x \phi_\sigma(j)] S_j^z + \frac{J}{4\pi\lambda} \sum_j \{ \cos[\phi_\sigma(j)] \\
& + \cos[2k_F j + \phi_\rho(j)] \} (e^{-i\theta_\sigma(j)} S_j^+ + \text{H.c.}) \\
& - \frac{J}{2\pi\lambda} \sum_j \sin[\phi_\sigma(j)] \sin[2k_F j + \phi_\rho(j)] S_j^z. \quad (3)
\end{aligned}$$

This equation has the same form as for a standard Kondo lattice<sup>3</sup> except that (i) we have to keep in mind that the impurity spin, i.e., terms containing  $S_j^z$ ,  $S_j^+$ , and  $S_j^-$ , contribute only if there is an  $f$  spin at site  $j$ , and (ii) the even cutoff function  $\Lambda(k)$ , defined in Eq. (2), satisfying  $\Lambda(k) \approx 1$  for  $|k| < 1/\lambda$  and  $\Lambda(k) \approx 0$  otherwise, is needed in the Bose fields to ensure that delocalized conduction electrons are described. Delocalization is essential to describe ferromagnetism,<sup>3,4</sup> since ferromagnetism in the Kondo lattice models is due to the double exchange, which only requires that  $N_c < N_f$ .<sup>10</sup>

In this situation each electron has on average more than one localized spin to screen, and since hopping between localized spins is energetically most favorable for electrons which preserve their spin as they hop, this tends to align the underlying localized spins.<sup>10</sup> This also means that double exchange will vanish if the distance between impurity spins is larger than  $\lambda$ . At lengths beyond  $\lambda$  the electrons will behave as collective density fluctuations, as usual in one-dimensional systems.<sup>8</sup> Hence,  $\lambda$  measures the effective range of the double exchange, and, in principle, it is a function of  $J$ ,  $n_c$ , and  $n_f$ .

The most straightforward method to determine an ordering of the localized spins is by applying a unitary transformation  $\tilde{H} = e^{\hat{S}} H e^{-\hat{S}}$ . We choose the transformation which changes to a basis of states in which the conduction-electron spin degrees of freedom are coupled directly to the localized spins  $\hat{S} = i(J/2\pi v_F) \sum_j \theta_\sigma(j) S_j^z$ . We perform the unitary transformation up to infinite order, so there is not any artificial truncation error generated (for details see Ref. 3). In the new transformed basis the double-exchange interaction leading to ferromagnetism is clearly exhibited and we obtain the effective Hamiltonian for the localized spins:

$$\begin{aligned}
H_{\text{eff}} = & - \frac{J^2}{2\pi^2 v_F} \sum_{i,j} \frac{\lambda}{\lambda^2 + (i-j)^2} S_i^z S_j^z \\
& + \frac{J}{2\pi\lambda} \sum_i \{ \cos[K(i)] + \cos[2k_F i] \} S_i^x \\
& - \frac{J}{2\pi\lambda} \sum_i \sin[K(i)] \sin[2k_F i] S_i^z. \quad (4)
\end{aligned}$$

$K(j)$  originates from the unitary transformation  $K(j) = i(J/2\pi v_F) \sum_{j'} [\phi_\sigma(j), \theta_\sigma(j')] S_{j'}^z$ , with  $[\phi_\sigma(j), \theta_\sigma(j')] = i\pi \text{sgn}(j-j')$ . Thus,  $K(j)$  counts all the  $S_{j'}^z$ 's to the right of the site  $j$  and subtracts from those to the left of  $j$ :  $K(j) = (J/2\pi v_F) \sum_{j'} (S_{j+j'}^z - S_{j-j'}^z)$ . This term gives the crucial difference between KLM and DKLM, as will be explained later on. The most important term in Eq. (4) is the first one, which clearly shows that a ferromagnetic coupling emerges for DKLM. This coupling is non-negligible for  $N_c < N_f$  and  $i-j \leq \lambda$  and its strength will decrease with increasing distance between impurity spins.

For  $N_c < N_f$ , the physical picture given by Eq. (4) will be crucially different if the lattice of impurity spins contains commensurate or incommensurate array of holes. Hence, we analyze these two cases separately. If we have a commensurate doping of the impurity spins, then we can approximate the ferromagnetic term in the usual way by taking  $\approx 1/n_f$  for the shortest average distance between  $f$  spins:  $\{ J^2 n_f^2 \lambda / [2\pi^2 v_F (1 + n_f^2 \lambda^2)] \} \sum_i S_i^z S_{i+1/n_f}^z$ . Lattice sites which are not occupied by  $f$  spins are inert and do not contribute to the ferromagnetic phase. This was verified by DMRG: the calculated  $f$ - $f$  spin correlation functions behave similarly as those of the normal KLM. The  $f$ -structure factor has the usual peak at  $k/\pi = N_c/N_f$  for low  $J$ , hence in the commensurate case the DKLM behaves similar to the standard KLM model.

To understand the behavior of the second and to third term from Eq. (4), we notice that  $K(i)$  is vanishingly small for the commensurate case, as the number of  $f$  impurity spins to the left and to the right of a given site  $i$  is the same. So the effective Hamiltonian will reduce to the random transverse field Ising model, as in the KLM.<sup>3</sup> The randomness is generated by  $[1 + \cos(2k_F i)]$  at large distances and it is driven by a cosine distribution, similar to spin glasses.<sup>11</sup> To determine the phase transition we need the dependence  $\lambda = \lambda(J, n_c, n_f)$ , which however is very difficult to determine, and as such we use the low density value  $\lambda \approx \sqrt{2/J}$  close to criticality, similar to previous works.<sup>3,12</sup> In this way we obtain the critical phase transition line to be  $J = \pi \sin(\pi n_c/2) / [1 - \pi \sin(\pi n_c/2)/n_f^2]$ , which represents a quantum order-disorder transition with variable exponents.<sup>3</sup> However, this ferromagnetic phase disappears for larger distances between impurities because, as mentioned earlier, the double-exchange interaction vanishes if the average distance between impurity spins,  $1/n_f$ , is larger than  $\lambda$ . This is very important because it ensures that the single-impurity limit  $n_f \rightarrow 0$  is free of ferromagnetism, as it should be.

The incommensurate case is more difficult than the commensurate case. The reason is that in the low concentration limit the properties of DKLM will be very much dependent on the random distribution of  $f$  spins. We may observe phase separation or clusterization processes in this case. In this limit, where the average distance between impurities is very large, then the single-impurity<sup>2</sup> approximation seems natural. However, if we look at small doping of  $f$  electrons only, then the main difference compared to the commensurate limit studied previously is that the  $K(j)$  term, in Eq. (4), is not negligible anymore. The impurity  $f$  spins are no longer equally distributed to the left and right of a given site  $j$ . However, for small doping of  $f$  electrons the main contribution to  $K(j)$ , namely, to  $\sum_{j'}(S_{j+j'}^z - S_{j-j'}^z)$ , is given by the few number of uncompensated (free) spins,  $S_{\text{free}}^z$ . Hence, we write  $S_{\text{free}}^z \approx \sum_{j'}(S_{j+j'}^z - S_{j-j'}^z) = 2\sum_{j', j' > j} S_{j'}^z - \sum_{j'} S_{j'}^z$ . Noting that  $\pm 2iS^z \equiv \exp(\pm i\pi S^z)$ , we have  $K(j) \approx (J/2v_F)\exp(2i\pi\sum_{j', j' > j} S_{j'}^z)$ . Hence  $K(j) \approx (-1)^j (J/2v_F)$ , which gives rise to a staggered field. The properties of Eq. (4) are then given by the staggered field Ising model, which gives an antiferromagnetic ordering. This antiferromagnetic ordering of the impurity spins represents a new element in DKLM compared to the Kondo lattice. This corresponds to the soliton lattice obtained by Schlottmann in a dynamical mean-field treatment of the three-dimensional dilute Kondo lattice.<sup>13</sup>

Similar behavior also occurs above half filling, i.e.,  $N_c > N_f$ , where double exchange (as shown previously) does not appear. But bosonization still works: the effective Hamiltonian reduces to the second and third terms of Eq. (4), from which the most dominant term, for low doping of impurity spins, as in the case described previously, is a staggered  $S_i^z$  field. As the first term in Eq. (4) is missing in this case, the only fluctuation which can destroy a locked staggered order is  $S_i^x$ . For large  $J$  ( $4 \lesssim J$ ) the staggered order wins, while for smaller values of  $J$  the systems will be disordered.

As we approach half filling from both sides, the bosonization approach breaks down as the strongly oscillating (umklapp) fields start dominating. The DKLM will undergo a metal-insulator transition as in a standard quantum sine-Gordon model<sup>14</sup> by dynamical mass generation and a spin gap will also appear. This can be understood easily, because the half-filled DKLM is equivalent to the quarter-filled periodic Anderson model, which has an antiferromagnetic order.<sup>12</sup> The only difference from the Kondo lattice is that the massive solitons obtained for DKLM are of Su, Schrieffer, and Heeger type.<sup>15</sup> However, in the case of DKLM the presence of the spin gap will cause short-range antiferromagnetic correlations to appear rather than a true long-range order.

To confirm the previously obtained magnetic phases, we performed non-Abelian DMRG (Ref. 7) analysis of the DKLM model in the commensurate case, for both the  $N_c < N_f$  and  $N_c > N_f$ , where ferromagnetism and antiferromagnetism, respectively, exist. The SO(4) symmetry of the Kondo lattice survives into the dilute model, thus we use basis states labeled by the total spin and total pseudospin. This allows us to determine the phase diagram by directly measuring the energy crossover of the polarized and singlet

symmetry sectors, a technique which is not available when using just the  $z$ -component of spin.

For the  $N_c < N_f$  case, we have investigated several commensurate dilution patterns of the form “00f00f00f . . .”; “0f0f0f0f . . .”; and “0ff0ff0ff . . .” in a 64-site long chain. While in the  $N_c > N_f$  limit we have studied the  $n_f = 0.8$  localized spin filling (to be in accordance with the bosonization requirement of low dilution) on a 80-site long DKLM chain, i.e., we investigated the pattern “0ffff0ffff . . .”

These patterns were selected in such a way that the chain middle-point reflection symmetry was preserved to accelerate the calculations. There was only one exception: the “0f0f0f” chain has an impurity in the middle, “0f0ff0f0,” but its effect is rather small compared to our final errors and so it was neglected. An important technique for performing efficient DMRG calculations is the wavefunction transformation to provide a good initial guess vector from one iteration to the next, first introduced by White.<sup>18</sup> However White’s transformation does not apply to the case of reflection-symmetric blocks. This is because the environment basis in the wavefunction transformation is always taken from the *previous* sweep, whereas use of reflection symmetry demands that the environment block is the spatial reflection of the system block obtained from the *current* sweep. The correct transformation is only obtained after determining the overlap between the previous and current basis vectors. This can be formulated as a minimization problem and solved via a singular-value decomposition. This calculation is presented in the Appendix.

In the DMRG calculations careful error and convergence analyses were used, and we extrapolated the energy linearly to zero truncation error (we saw no quadratic terms large enough to affect the fit). For each given dilution pattern, filling  $N_c/N_f$ , and interaction constant  $J$ , we used several DMRG sweeps of between 200 and 400 SO(4)-symmetric states.<sup>16</sup>

For  $N_c < N_f$  ferromagnetism appears at large  $J$  values, see Fig. 1. A point on the phase diagram shown in Fig. 1 is judged to be ferromagnetic if the extrapolated energy of the spin  $S_{\text{max}}$  run is lower than the spin zero energy. This energy difference to the spin-singlet excited state can be calculated directly using the SO(4) basis set of the non-Abelian DMRG. The phase transition line can be determined with high accuracy if one plots the energy gap between the spin  $S_{\text{max}}$  and spin zero states as a function of  $J$ —the gap rapidly decreases as the transition is approached. It should be mentioned that, as well as in the standard Kondo case,<sup>4</sup> there also exists additional ferromagnetic phases inside the paramagnetic region for dilute Kondo chains.

In the opposite limit, i.e.,  $N_c > N_f$ , we have confirmed the existence of short antiferromagnetic fluctuations by calculating the spin structure factor  $S(k)$ , the Fourier transform of  $S(x) \equiv \langle S_0^z S_x^z \rangle$ , where  $x$  is measured in units of the lattice constant. As can be seen in Fig. 2, for small  $J$  the peak in  $S(k)$  is at  $2k_F$  (similar to KLM, Ref. 4), i.e., the DKLM is a disordered paramagnet. The dominant  $2k_F$  backscattering processes are manifest of a system of free localized spins embedded in effective fields determined by conduction-

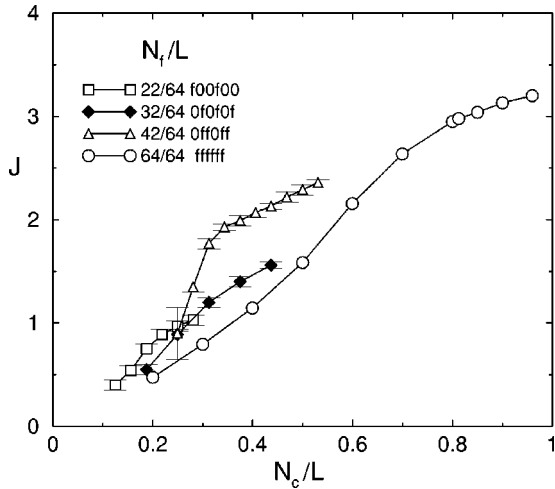


FIG. 1. The phase diagram of the dilute Kondo model in different commensurate filling cases for  $N_c < N_f$ . Legend shows patterns of dilution. Open circles correspond to the standard KLM model. The system of a given dilution pattern is ferromagnetic above the corresponding solid line and paramagnetic below.

electron scattering. As we increase  $J$ , a distinctive peak at  $k = \pi$  appears (see Fig. 2), thus DKLM exhibits an antiferromagnetic signal. However, this signal is broadened by the presence of the spin and charge gaps of the conduction electrons, as argued earlier. Simultaneously with the emergence of the  $k = \pi$  peak, the  $2k_F$  peak starts to broaden, and as we further increase  $J$  decreases in strength to the point that it vanishes.

To further investigate this antiferromagnetic signal we performed an additional DMRG calculation for  $n_f = 0.8$  and electron filling  $n_c = 0.9$  at  $J/t = 3$ , with 1000 states kept, but treating the localized spins as separate lattice sites. This sacrifices some accuracy for a significant improvement in efficiency. Due to the matrix product structure of the wave function obtained by DMRG, correlation functions inevitably decay exponentially at long distances.<sup>19</sup> By choosing larger system sizes (the largest studied size was  $L = 600$ ) that are long compared with the “truncation length” imposed by the DMRG, the effect of open boundaries is minimized. Thus the relevant length parameter for the calculation is not the system size itself, but rather the truncation length of the DMRG. This makes finite-size scaling analysis problematic, however we believe that within the accuracy of the overall calculation, the obtained wave function is sufficiently close to the thermodynamic limit that such analysis would not provide additional information.

The obtained wave function agrees with the result from the shorter length chains, namely, the main feature is a peak in the structure factor at  $k = \pi$ , corresponding to exponential decay with a correlation length of  $29 \pm 3$  lattice spacings, see Fig. 3. Here in comparison to the exponential decay (continuous lines) we also show a power-law decay (dashed curves). The plot clearly shows that the best fit of the data is an exponential function. Thus the antiferromagnetic correlation length is always finite, which seems to indicate that this regime is a continuation of the spin liquid state of the half-filled Kondo lattice.<sup>17</sup> However, the spin and charge gaps are

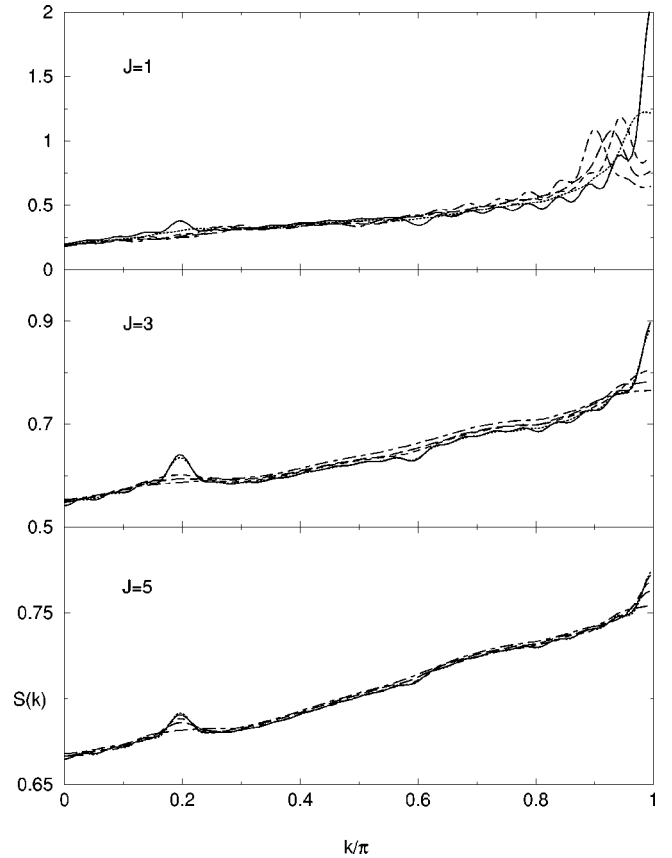


FIG. 2. Typical  $J$  dependences of the conduction electron spin structure factor  $S(k)$  for  $n_f = 0.8$  and  $n_c = 1$ , continuous,  $n_c = 0.975$ , dotted,  $n_c = 0.95$ , dashed,  $n_c = 0.925$ , long dashed, and  $n_c = 0.90$ , dot-dashed curves.

much smaller than in the usual KLM. Indeed, direct measurement of the gaps has proven problematic, even for relatively small systems, hence there is a possibility of power-law decay of the spin-spin correlation function for large enough distances with the vanishing of the spin gap.

In conclusion, we have studied the dilute Kondo lattice model in one dimension both numerically, using DMRG, and analytically, with a standard bosonization approach. We have derived an effective Hamiltonian for the  $f$  spins, which accounts for the appearance of a ferromagnetic phase seen with a commensurate dilution pattern of the impurity spin array. The paramagnetic-ferromagnetic phase transition shifts to higher coupling  $J$  values as the  $f$  spins of the chain are diluted, in agreement with the numerical DMRG calculation. We have also shown that within the paramagnetic phase of the incommensurate dilution limit or above half filling, i.e.,  $N_c > N_f$  for low doping of impurity spins, strong short-range antiferromagnetic correlations are found. This distinguishes the dilute Kondo lattice model from the standard Kondo lattice model.

#### ACKNOWLEDGMENTS

Work in Australia was supported by the Australian Research Council and Department of Industry, Science and Resources Work in Sweden was supported by the Swedish

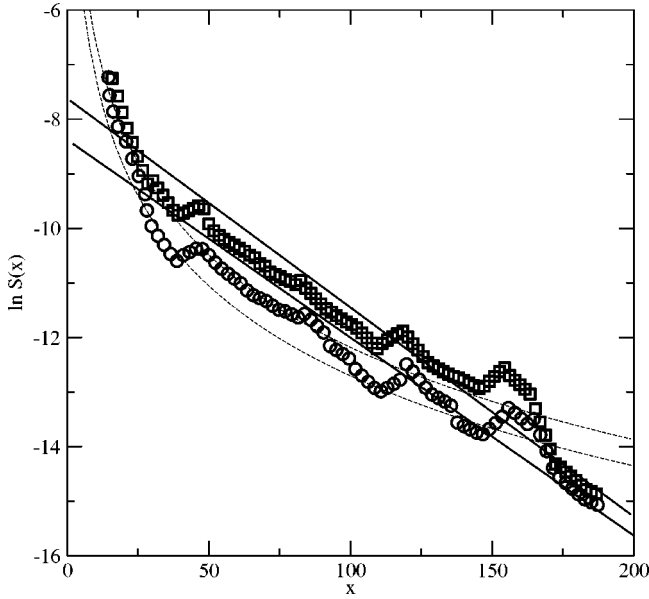


FIG. 3. The logarithm of the spin-spin correlation function  $S(x)$  for the  $f$  (squares) and  $c$  (circles) electrons for  $J=3$ ,  $n_f=0.8$ ,  $n_c=0.9$ , and  $L=600$  with 1000 states kept. The continuous lines are the best linear fit, while the dashed lines are the best logarithmic fit.

Natural Science Research Council (Vetenskapsrådet), the Swedish Foundation for International Cooperation in Research and Higher Education (STINT), and the Swedish Foundation for Strategic Research (SSF). Work in The Netherlands was supported by the Foundation for Fundamental Research on Matter (FOM) and The Netherlands Organization for Scientific Research (NWO). Most of the numerical calculations were performed at National Facility of the Australian Partnership for Advanced Computing.

## APPENDIX

In this appendix, the basis transformation required to obtain an initial wave function at the midpoint of a reflection-symmetric DMRG calculation is derived. At the midpoint, the wave function can be written in matrix form as a tensor product of left and right basis states, first for the wave function at the previous sweep,

$$|\Psi\rangle = \sum_{a'a} (\psi_{a'a}) |a'\rangle |a\rangle, \quad (\text{A1})$$

where the left-block basis states  $|a'\rangle$  are the spatial reflection of the right-block basis states  $|a\rangle$ . The wave function, at the end of the standard transformation,<sup>18</sup> is given in a mixed basis as

$$|\Phi\rangle = \sum_{ba} (\psi_{ba}) |b\rangle |a\rangle, \quad (\text{A2})$$

which is the tensor product of the left- (system) block basis of the current sweep with the right- (environment) block basis of the previous sweep. The task is to find a transformation  $T=(t_{ba})$  which gives the correspondence between the two

basis sets, thereby allowing the wave function to be determined in the  $b$  basis only, as required for the DMRG algorithm when reflection symmetry is used.

The required transformation maximizes the overlap between the wave function at the current and the wave function at the previous sweep. The dimension of the  $|a\rangle$  and  $|b\rangle$  basis sets,  $N_a$  and  $N_b$ , respectively, are not necessarily the same, thus  $T$  is not in general a square matrix.

We consider the case  $N_b \leq N_a$ , but the proof for  $N_b > N_a$  proceeds similarly. The rows of  $T$  can be constrained to be orthogonal and normalized via a set of Lagrange multipliers  $\lambda_{a'a'}/2$ , represented as a matrix which can be taken to be symmetric. Thus the maximization problem is

$$F = \sum_{a,a',b} \phi_{ba} T_{ba'} \psi_{aa'} - \sum_{b'b} \frac{\lambda_{b'b}}{2} \sum_a (T_{b'a} T_{ba} - \delta_{b'b}). \quad (\text{A3})$$

Taking the partial derivative with respect to  $T_{\beta\alpha}$ , one obtains

$$\frac{\partial F}{\partial T_{\beta\alpha}} = \sum_{\alpha} \phi_{\beta\alpha} \psi_{\alpha\alpha} - \sum_b \lambda_{\beta b} T_{b\alpha}. \quad (\text{A4})$$

The solution of  $\partial F / \partial T_{\beta\alpha} = 0$  gives the desired transformation. Switching to matrix form

$$\Phi \Psi^\dagger = \Lambda T, \quad (\text{A5})$$

where  $\Lambda = (\lambda_{b'b})$  is an  $N_b \times N_b$  symmetric matrix,  $\Phi$  is an  $N_b \times N_a$  matrix,  $\Psi$  is an  $N_a \times N_a$  matrix, and  $T$  is an  $N_b \times B_a$  row-orthogonal matrix.

We now perform the singular-value decomposition of the left-hand side of Eq. (A5), giving

$$\Phi \Psi^\dagger = U D V^T, \quad (\text{A6})$$

where  $U$  is an  $N_b \times N_b$  orthogonal matrix,  $D$  is an  $N_b \times N_b$  diagonal matrix containing the singular values, and  $V^T$  is an  $N_b \times N_a$  row-orthogonal matrix. The singular-value decomposition of the right-hand side of Eq. (A5) is performed for  $\Lambda$  and  $T$  separately, giving

$$\Lambda T = U D_\Lambda W^T X D_T V^T, \quad (\text{A7})$$

where  $D_\Lambda$  is an  $N_b \times N_b$  diagonal matrix containing the singular values of  $\Lambda$ ,  $W^T$  is a  $N_b \times N_b$  orthogonal matrix,  $X$  is an  $N_b \times N_b$  orthogonal matrix, and  $D_T$  is an  $N_b \times N_b$  diagonal matrix containing the singular values of  $T$ . Now  $\Lambda$  is symmetric, therefore the singular-value decomposition reduces to a similarity transformation, giving  $W=U$ . But  $T$  is row orthogonal, therefore the singular values are identically equal to 1, giving  $D_T=I$ . Thus the singular values of  $\Lambda$  must coincide with the singular values of  $\Phi \Psi^\dagger$ , implying  $D_\Lambda=D$ . Thus,

$$\Phi \Psi^\dagger = U D V^T = U D U^T X V^T, \quad (\text{A8})$$

which implies that  $X=U$ . Thus, from the singular-value decomposition of  $T$ ,

$$T = X D_T V^T = U V^T, \quad (\text{A9})$$

where  $U$  and  $V^T$  are given by the decomposition of  $\Phi \Psi^\dagger$  in Eq. (A6).

- \*Present address: Instituut Lorentz for Theoretical Physics, Leiden University, P.O. Box 9506, NL-2300 RA Leiden, The Netherlands.
- <sup>1</sup>See, for example, P.A. Lee, T.M. Rice, J.W. Serene, L.J. Sham, and J.W. Wilkins, *Comments Condens. Matter Phys.* **12**, 99 (1986); P. Fulde, J. Keller, and G. Zwicknagl, in *Solid State Physics: Advances in Research and Applications* (Academic Press, New York, 1988), Vol. 41, p. 1.
- <sup>2</sup>P.W. Anderson, G. Yuval, and D.R. Hamann, *Phys. Rev. B* **1**, 2719 (1989); N. Andrei, *Phys. Rev. Lett.* **45**, 379 (1980); N. Andrei, K. Furuya, and J.H. Lowenstein, *Rev. Mod. Phys.* **55**, 331 (1983).
- <sup>3</sup>G. Honner and M. Gulacsi, *Phys. Rev. Lett.* **78**, 2180 (1997); *Phys. Rev. B* **58**, 2662 (1998).
- <sup>4</sup>I.P. McCulloch, M. Gulacsi, S. Caprara, A. Juozapavicius, and A. Rosengren, *J. Low Temp. Phys.* **117**, 323 (1999); I.P. McCulloch, A. Juozapavicius, A. Rosengren, and M. Gulacsi, *Philos. Mag. Lett.* **81**, 869 (2001); *Phys. Rev. B* **65**, 052410 (2002).
- <sup>5</sup>M. Troyer and D. Würtz, *Phys. Rev. B* **47**, 2886 (1993); H. Tsunetsugu, M. Sigrist, and K. Ueda, *ibid.* **47**, 8345 (1993); S. Moukouri and L.G. Caron, *ibid.* **52**, R15 723 (1995); M. Guerrero and C.C. Yu, *ibid.* **51**, 10 301 (1995); C.C. Yu and M. Guerrero, *ibid.* **54**, 8556 (1996); S. Caprara and A. Rosengren, *Europhys. Lett.* **39**, 55 (1997).
- <sup>6</sup>H. Tsunetsugu, M. Sigrist, and K. Ueda, *Rev. Mod. Phys.* **69**, 809 (1997); N. Shibata and K. Ueda, *J. Phys.: Condens. Matter* **11**, R1 (1999).
- <sup>7</sup>I.P. McCulloch and M. Gulacsi, *Aust. J. Phys.* **53**, 597 (2000); *Philos. Mag. Lett.* **81**, 447 (2001); *Europhys. Lett.* **57**, 852 (2002).
- <sup>8</sup>F.D.M. Haldane, *J. Phys. C* **14**, 2585 (1981). For a review, see J. Voit, *Rep. Prog. Phys.* **57**, 977 (1994); M. Gulacsi, *Philos. Mag. B* **76**, 731 (1997); J. von Delft and H. Schöller, *Ann. Phys.* **4**, 225 (1998).
- <sup>9</sup>S. Mandelstam, *Phys. Rev. D* **11**, 3026 (1975); T. Banks, D. Horn, and H. Neuberger, *Nucl. Phys. B* **108**, 199 (1976); see also Y.K. Ha, *Phys. Rev. D* **29**, 1744 (1984).
- <sup>10</sup>C. Zener, *Phys. Rev.* **82**, 403 (1951); P.W. Anderson and H. Hasegawa, *ibid.* **100**, 675 (1955).
- <sup>11</sup>A.A. Abrikosov, *Adv. Phys.* **29**, 869 (1980).
- <sup>12</sup>T. Yanagisawa and M. Shimoi, *Int. J. Mod. Phys. B* **10**, 3383 (1996).
- <sup>13</sup>P. Schlottmann, *Phys. Rev. B* **46**, 998 (1992).
- <sup>14</sup>M. Gulacsi and K.S. Bedell, *Phys. Rev. Lett.* **72**, 2765 (1994).
- <sup>15</sup>S.W. Su, J.R. Schrieffer, and A.J. Heeger, *Phys. Rev. B* **22**, 2099 (1980).
- <sup>16</sup>Note that each block state of our non-Abelian DMRG corresponds to several ordinary DMRG states, since it is a spin multiplet rather than an individual state (see Ref. 7).
- <sup>17</sup>R. Jullien and P. Pfeuty, *J. Phys. F: Met. Phys.* **11**, 353 (1981); H. Tsunetsugu, Y. Hatsugai, K. Ueda, and M. Sigrist, *Phys. Rev. B* **46**, 3175 (1992); C.C. Yu and S.R. White, *Phys. Rev. Lett.* **71**, 3866 (1993); M. Guerrero and C.C. Yu, *Phys. Rev. B* **51**, 10 301 (1995).
- <sup>18</sup>S.R. White, *Phys. Rev. Lett.* **77**, 3633 (1996).
- <sup>19</sup>S. Rommer and S. Östlund, *Phys. Rev. B* **55**, 2164 (1997).